Int. J. Heat Mass Transfer. Vol. 31, No. 8, pp. 1619–1626, 1988
Printed in Great Britain

0017-9310/88 \$3.00+0.00

Non-linear stability of forced vapour flow condensation

MAZHAR ÜNSAL†

Department of Mechanical Engineering, University of Hawaii at Manoa, Honolulu, Hawaii, U.S.A.

(*Received* 1 *May* 1987 *and in final form* 9 *December* 1987)

Abstract—Non-linear stability of a liquid condensate film flowing on an inclined isothermal surface and adjacent to a flowing pure vapour is investigated by the method of multiple scales. Results from the analysis are discussed for the special cases of forced flow steam condensation on vertical surfaces, under horizontal surfaces, and above horizontal surfaces. It is found that increasing cocurrent steam velocity has a stabilizing effect on thin condensate films flowing on vertical surfaces and under horizontal surfaces when the vapour velocities are small. It is also found that thin condensate films flowing above horizontal surfaces under the action of cocurrent low velocity forced steam flow are stable with respect to both infinitesimal and finite amplitude disturbances but become unstable at high vapour velocities.

INTRODUCTION

CONDENSATION heat transfer is important in power plant systems, refrigeration equipment and many other industrial processes. Condensation of pure quiescent saturated vapours on flat isothermal surfaces have been studied by Nusselt [1], Rohsenow [2], Sparrow and Gregg [3], Chen [4], and Koh *et al.* [5]. Analyses of steady-state condensation of flowing pure saturated vapours on flat isothermal surfaces were reported by Shekriladze and Gomelauri [6], Denny and Mills [7], and Koh [8]. Steady condensate film flow and heat transfer as determined from steady-state theoretical investigations were later subjected to hydrodynamic stability analyses. Linearized stability studies of condensate films flowing under the action of gravity on flat isothermal walls were reported in refs. [9–12]. All of these investigations of linearized stability characteristics of condensate films are limited to disturbances having infinitesimal amplitudes and become invalid as the amplitude of the disturbances become finite. Stability characteristics of finite amplitude disturbances on condensate films have also been studied previously by means of a non-linear stability analysis [13]. It was found from results of this non-linear stability analysis that linearly unstable small disturbances on a vertical wall reach finite equilibrium amplitudes when the Reynolds number is small. It was also found that small but finite amplitude disturbances in the linearly stable region of the α–*Re* plane are also stable according to the non-linear theory.

All of the stability analyses of film condensation reported in refs. [9–13] are limited to the special case of quiescent vapour condensation. Reference [14] presented a linearized stability analysis of a condensate film adjacent to a flowing pure saturated vapour.

The purpose of this theoretical study is the extension of the analysis presented in ref. [14] to the study of the characteristics of finite amplitude disturbances on a condensate film flowing over an inclined isothermal surface and adjacent to a flowing pure saturated vapour. The first-order perturbation solution for the dimensionless temperature distribution as well as the problem formulation are directly adapted from that given in ref. [14]. The present study corresponds to a non-linear stability analysis of condensate films as determined by steady-state analyses reported in refs. [4–8]. Results are discussed for the particular cases of forced vapour flow condensation of steam on vertical surfaces, above horizontal surfaces, and under horizontal surfaces.

DERIVATION OF THE STABILITY PROBLEM

Saturated vapour at temperature $\tilde{T}_s$ flowing with free stream vector velocity $\mathbf{V}_v$ next to a condensate film on an inclined isothermal plane surface at temperature $\tilde{T}_w$ is considered (Fig. 1). A constant free stream $\tilde{x}$-component vapour velocity, $\tilde{U}_{v0}$, is assumed in accordance with previous steady-state analyses of the problem. This is an idealized free stream condition and will not correspond to the actual physical situation in most practical applications. All of the previous steady-state analyses of the problem [4–8] were based on this free stream condition. The present study is an investigation of the stability of the flows reported in refs. [4–8] and, consequently, the same vapour free stream condition is retained.

Almost all of the previous studies of the stability of film condensation are based on the parallel flow approximation and effects of nonparallelism in the base flow are also neglected in the present analysis. The interfacial mass, momentum and energy conditions across the liquid–vapour interface during forced vapour condensation were formulated in ref. [14] for the case of negligibly small vapour hydrodynamic boundary layer thickness and the dimensionless prob-

† On leave from Department of Mechanical Engineering, University of Gaziantep, 27310 Gaziantep, Turkey.

NOMENCLATURE

A	complex wave amplitude
a	wave amplitude
c	complex wave velocity, $c_r + ic_i$
c_{i1}, c_{i3}	wave amplification rate coefficients
c_{r1}, c_{r3}	wave velocity coefficients
F	acceleration effect parameter, $(c_p\Delta T/h_{fg})Pr$
g	gravitational acceleration
$\tilde{L}$	length of plate
L	$\tilde{L}/(2\nu^2/g)^{1/3}$
L_1, L_2	differential operators given in Appendix B
N	$2^{1/3}\sigma/\rho\nu^{4/3}g^{1/3}$
Pr	Prandtl number
R	$g\tilde{\eta}_0^3/2\nu^2$
$\tilde{t}, t$	dimensional, dimensionless time
T_0, T_1, T_2	multiple time scales
$\tilde{T}, \tilde{T}_s, \tilde{T}_w$	liquid, vapour, wall temperatures
u	$\tilde{U}_{v0}/(g\nu/2)^{1/3}$
$\tilde{U}_v$	vapour $\tilde{x}$-component velocity
$\tilde{U}_0$	characteristic velocity, $g\tilde{\eta}_0^2/2\nu$
$\tilde{U}_{v0}$	base flow $\tilde{x}$-component velocity
U	$\tilde{U}_{v0}/\tilde{U}_0$
$\tilde{V}_v$	vapour $\tilde{y}$-component velocity
$\tilde{V}_{v0}$	base flow $\tilde{y}$-component velocity
V	$-\tilde{V}_{v0}/\tilde{U}_0$
$(\tilde{x}, \tilde{y}), (x, y)$	dimensional, dimensionless Cartesian coordinates.

Greek symbols

α	wave number, $2\pi\tilde{\eta}_0/\lambda$
γ	ρ_v/ρ
ε	small parameter
$\tilde{\eta}$	film thickness
$\tilde{\eta}_0$	time averaged base flow film thickness
$\bar{\eta}$	dimensionless base flow film thickness
η	dimensionless disturbance film thickness
θ	dimensionless liquid temperature
λ	wavelength
ν	liquid kinematic viscosity
ρ, ρ_v	liquid, vapour density
σ	surface tension
ϕ	angle of inclination
$\tilde{\Phi}$	vapour potential function
Φ	dimensionless vapour disturbance potential function
Ψ	dimensionless liquid stream function.

Subscripts

$x, y, z, t, T_0, T_1, T_2$ partial differentiation with respect to the subscript.

Dimensionless terms

t	$\alpha\tilde{U}_0\tilde{t}/\tilde{\eta}_0$
x	$\alpha\tilde{x}/\tilde{\eta}_0$
y	$y/\tilde{\eta}_0$
z	αy
η	$\tilde{\eta}/\tilde{\eta}_0$
Φ	$\alpha\tilde{\Phi}/\tilde{U}_0\tilde{\eta}_0$.

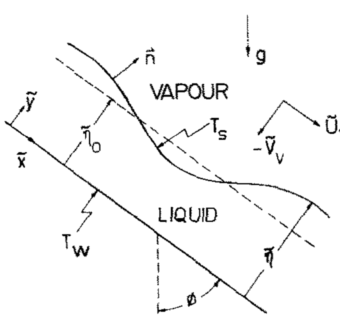

FIG. 1. Geometry of the separated two-phase flow.

lem formulation was analysed by means of an asymptotic expansion valid for small wave numbers leading to a first-order asymptotic solution for the liquid stream function and the liquid temperature distribution. The problem formulation is given by equations (20)–(33) of ref. [14]. It is noted here that this problem formulation is based on a generalized version of the so called 'asymptotic shear stress interfacial condition' which is represented by interfacial condition (28) of ref. [14]. The derivation of this interfacial condition is obtained via neglect of vapour boundary layer and by balancing the liquid shear stress with the momentum flux across the interface. Negligence of the vapour boundary layer is a valid approximation at high condensation rates. When the condensation rate is high, the vapour hydrodynamic boundary layer thickness becomes thin and it then becomes possible to study the non-linear stability problem by considering the coupled system of the condensate film and the free stream vapour flow. The interfacial condition (28) reported in ref. [14] corresponds to and is in agreement with equation (4) of ref. [6] and equation (5) of ref. [7].

A first-order asymptotic solution of the non-linear stability problem with respect to the dimensionless wave number is given by equations (37)–(45) of ref. [14]. Substitution of this solution into interfacial conditions (30) and (31) of ref. [14] yields an interfacial mass conservation condition (equation (46) of ref. [14]) and an interfacial energy conservation condition (equation (47) of ref. [14]). The stability problem was then obtained by separating the film thickness and the vapour free stream potential function into base flow and disturbance components. The procedure reported in ref. [14] leads to the following base flow and non-linear stability problems.

The base flow problem:

(a) interfacial energy condition

$$k_0/\bar{\eta}-k_2\bar{\eta}^2\bar{\eta}_x-k_3U\bar{\eta}_x+\varepsilon^2S_2=\frac{\mathrm{d}}{\mathrm{d}x}\{k_5\bar{\eta}^3\bar{\eta}_x+k_9\bar{\eta}^3\bar{\eta}_{xxx}+k_{10}\bar{\eta}_x+k_{13}U^2\bar{\eta}^2\bar{\eta}_x-k_{15}\bar{\eta}^6\bar{\eta}_x-k_{16}U\bar{\eta}^4\bar{\eta}_x\}+O(\alpha^3); \quad (1)$$

(b) interfacial mass condition

$$j_0/\bar{\eta}-j_2\bar{\eta}^2\bar{\eta}_x-j_3U\bar{\eta}_x-V+\varepsilon^2S_1+O(\alpha^2)=0. \quad (2)$$

The non-linear stability problem:

(a) disturbance vapour motion and conditions at $z=\infty$

$$\Phi_{xx}+\Phi_{zz}=0 \quad (3)$$

$$\Phi_x=\Phi_z=0 \quad \text{at } z=\infty; \quad (4)$$

(b) interfacial energy condition valid at $z=0$

$$k_0\eta+k_1\eta_t+k_{17}\eta_x+k_{18}\eta_{xx}+k_9\eta_{xxxx}+k_{19}\eta_{xt}+k_3\Phi_{xx}+k_{20}\Phi_{xxz}-k_{21}\Phi_{xxx}-k_8\Phi_{xxt}$$
$$=\varepsilon\left\{-S_2+k_0\eta^2-2k_2\eta\eta_x-k_3\eta_x\Phi_x-k_{29}\eta_x\Phi_{xz}-k_3\eta_x\Phi_{xx}-2\alpha k_3\eta\Phi_{xxz}+\frac{\partial}{\partial x}[k_{30}\eta\eta_x+k_{31}\eta\Phi_{xx}+k_6\Phi_x\Phi_{xx}-k_7\Phi_z\Phi_{xz}+3Vk_7\eta\Phi_{xz}+3k_8\eta\Phi_{xt}-3k_9\eta\eta_{xxx}+k_{32}\eta\eta_t-k_{11}\eta_t\Phi_x+k_{33}\eta_x\Phi_x]\right\}$$
$$+\varepsilon^2\left\{-k_0\eta^3-k_2\eta^2\eta_x-\alpha k^3\eta\eta_x\Phi_{xz}-\alpha k_3\eta^2\Phi_{xxz}-k_4\eta\eta_x\Phi_{xz}+\frac{\partial}{\partial x}[k_{34}\eta^2\eta_x+3k_6\eta\Phi_x\Phi_{xx}+k_{35}\eta^2\Phi_{xx}-3k_7\eta\Phi_z\Phi_{xz}+3k_7V\eta^2\Phi_{xz}+3k_8\eta^2\Phi_{xt}-3k_9\eta^2\eta_{xxx}+k_{36}\eta^2\eta_t-2k_{11}\eta\eta_t\Phi_x+k_{37}\eta\eta_x\Phi_x-k_{13}\eta_x\Phi_x^2]\right\}+O(\varepsilon^3)+O(\alpha^3); \quad (5)$$

(c) interfacial mass condition valid at $z=0$

$$j_0\eta+j_1\eta_t+(j_2+Uj_3)\eta_x+j_4\Phi_{xx}-\Phi_z-\alpha\Phi_{zz}$$
$$=\varepsilon\{-S_1+j_0\eta^2-2j_2\eta\eta_x-j_3\eta_x\Phi_x-j_4\eta\Phi_{xx}+\alpha\eta\Phi_{zz}\}+\varepsilon^2\{-j_0\eta^3-j_2\eta^2\eta_x\}+O(\alpha^2)+O(\varepsilon^3). \quad (6)$$

The non-linear terms in equations (5) and (6) were neglected in the linearized stability analysis reported in ref. [14]. Coefficients j_0–j_6, k_0–k_{28} and B_1–B_5 were reported in ref. [14]. The remaining coefficients are listed in Appendix A. In the above equations S_1 and S_2 correspond to effects of the finite amplitude disturbance on the base flow. The base flow problem will not be analysed in this study. A solution of the base flow problem for the special case of vanishing wave amplitude ($\varepsilon=0$) corresponding to steady forced vapour flow condensation is presented in ref. [15].

SOLUTION BY THE METHOD OF MULTIPLE SCALES

Interfacial mass condition (6) contains errors of the order of α^2 and ε^3. Analysis of the stability problem to second order with respect to the wave amplitude will therefore contain errors of the order of α^2 if the wave number and the wave amplitude are of the same order. It is therefore necessary to consider the wave number to be of the order of the square of the wave amplitude. Condition (6) will then be expressed in the following form:

$$j_0\eta-\Phi_z=\varepsilon(-S_1+j_0\eta^2)+\varepsilon^2(-j_0\eta^3-j_1\eta_t-j_5\eta_x-j_4\Phi_{xx}+\alpha\Phi_{zz})+O(\varepsilon^3) \quad \text{at } z=0. \quad (7)$$

Transformation from equation (6) into equation (7) is algebraically permissible noting that ε is a dummy variable and that this parameter will be replaced by unity at the end of the analysis.

In order to study the non-linear stability characteristics of waves having weak temporal amplification rates, the linear problem will be converted into a purely dispersive system by the introduction of

$$k_{17}=\bar{k}_{17}+\varepsilon\Gamma \quad (8)$$

into equation (5) where

$$\bar{k}_{17}=\bar{c}(k_1-j_0k_8)+j_0k_{21} \quad (9)$$

and $\bar{c}$ represents the wave speed corresponding to neutrally stable disturbances. The resulting stability problem will be analysed by the method of multiple scales [16]. Introducing multiple time scales given by

$$T_0=t, \quad T_1=\varepsilon t, \quad T_2=\varepsilon^2 t \quad (10)$$

the partial time derivative is transformed according to

$$\frac{\partial}{\partial t}\to\frac{\partial}{\partial T_0}+\varepsilon\frac{\partial}{\partial T_1}+\varepsilon^2\frac{\partial}{\partial T_2}. \quad (11)$$

Introduction of relation (11) and the following asymptotic expansions:

$$\Phi=\Phi_0+\varepsilon\Phi_1+\varepsilon^2\Phi_2+O(\varepsilon^3) \quad (12)$$

$$\eta=\eta_0+\varepsilon\eta_1+\varepsilon^2\eta_2+O(\varepsilon^3) \quad (13)$$

into equations (3)–(5) and (7) yields three problems corresponding to each order of ε. These problems are given in Appendix B. The dimensionless y-component vapour velocity has been eliminated from the stability problem given in Appendix B by substitution of $V = j_0 + \varepsilon^2 S_1$ from equation (2). The solution of the zeroth-order perturbation problem is a transverse disturbance with slow amplitude modulation given by

$$\eta_0 = A\,e^{iX} + \bar{A}\,e^{-iX} \tag{14}$$

$$\Phi_0 = -j_0\,e^{-z}\,\eta_0 \tag{15}$$

where $X = x - \bar{c}T_0$. $A = A(T_1, T_2)$ is the complex wave amplitude which is a function of the slow time scales. $\bar{A}$ is the complex conjugate of A. The zeroth-order wave speed is found to be

$$\bar{c} = -(k_{22} + j_0 k_{23})/k_{19}. \tag{16}$$

Substitution of the zeroth-order problem into the first-order problem and elimination of the steady terms in the interfacial energy condition yields

$$S_2 = 2k_0 A\bar{A}. \tag{17}$$

By this means, steady terms in the energy interfacial condition of the first-order problem are carried to equation (1) which is for the base flow film thickness. Application of the solvability condition to the first-order problem then yields

$$((j_0 k_8 - k_1) - ik_{19})\frac{\partial A}{\partial T_1} - i\Gamma A = 0. \tag{18}$$

The interfacial energy condition in the first-order problem given in Appendix B then becomes

$$L_1\eta_1 + L_2\Phi_1 = (k_{38} + ik_{39})A^2\,e^{i2X} + \mathrm{CC} \quad \text{at } z = 0 \tag{19}$$

where CC stands for the complex conjugate of the first term on the right-hand side. Steady terms in the interfacial mass condition of the first-order problem are carried to the steady part of the interfacial mass condition (equation (2)) by choosing

$$S_1 = 2j_0 A\bar{A}. \tag{20}$$

The interfacial mass condition in the first-order problem then takes the following form:

$$\Phi_{1z} = -j_0(A^2\,e^{i2X} + \mathrm{CC}) \quad \text{at } z = 0. \tag{21}$$

Solution for the Laplace equation and boundary conditions at $z = \infty$ given in the first-order problem reported in Appendix B together with conditions (19) and (21) is then obtained as

$$\eta_1 = bA^2\,e^{i2X} + \bar{b}\bar{A}^2\,e^{-i2X} \tag{22}$$

$$\Phi_1 = \tfrac{1}{2}j_0(1-b)\,e^{-2z}A^2\,e^{i2X} + \mathrm{CC} \tag{23}$$

where $b = b_r + ib_i$ is given in Appendix A and $\bar{b}$ is the complex conjugate of b. Substitution of equations (14) and (15) and equations (22) and (23) into the right-hand side of the second-order problem in Appendix B and application of the solvability condition now yields

$$(j_0 k_8 - k_1 - ik_{19})\frac{\partial A}{\partial T_2} + (k_{48} + ik_{49})A^2\bar{A} = 0. \tag{24}$$

Variation of the complex wave amplitude of the non-linear stability problem with respect to the slow time scales T_1 and T_2 are given by equations (18) and (24). Complex wave amplitude A will now be expressed by

$$A = \tfrac{1}{2}a\,e^{i\beta} \tag{25}$$

where $a(T_1, T_2)$ is a real function for the wave amplitude and $\beta(T_1, T_2)$ is a correction to the zeroth-order linear wave amplification rate, $\bar{c}$. Application of equation (25) to equations (18) and (24) gives

$$\frac{\partial a}{\partial T_1} = -\frac{k_{19}\Gamma}{(k_1 - j_0 k_8)^2 + k_{19}^2}a \tag{26}$$

$$\frac{\partial \beta}{\partial T_1} = -\frac{(k_1 - j_0 k_8)\Gamma}{(k_1 - j_0 k_8)^2 + k_{19}^2} \tag{27}$$

$$\frac{\partial a}{\partial T_2} = \frac{k_{19}k_{49} + (k_1 - j_0 k_8)k_{48}}{4((k_1 - j_0 k_8)^2 + k_{19}^2)}a^3 \tag{28}$$

$$\frac{\partial \beta}{\partial T_2} = -\frac{k_{19}k_{48} + (j_0 k_8 - k_1)k_{49}}{4((k_1 - j_0 k_8)^2 + k_{19}^2)}. \tag{29}$$

Noting that the wave amplification rate and the wave speed are given by

$$\frac{\mathrm{d}a}{\mathrm{d}t} = \varepsilon\frac{\partial a}{\partial T_1} + \varepsilon^2\frac{\partial a}{\partial T_2} \tag{30}$$

$$c_r = \bar{c} - \frac{\mathrm{d}\beta}{\mathrm{d}t} = \bar{c} - \left(\varepsilon\frac{\partial \beta}{\partial T_1} + \varepsilon^2\frac{\partial \beta}{\partial T_2}\right) \tag{31}$$

and utilizing equations (26)–(29) together with equation (8), one obtains

$$\alpha\frac{\mathrm{d}(\varepsilon a)}{\mathrm{d}t} = \alpha\{c_{i1} + c_{i3}(\varepsilon a)^2\}\varepsilon a \tag{32}$$

$$c_r = c_{r1} + c_{r3}(\varepsilon a)^2. \tag{33}$$

Here, αc_{i1} is the linear wave amplification rate and αc_{i3} is the coefficient of the non-linear wave amplification rate. c_{r1} is the linear wave velocity and c_{r3} is the coefficient of the non-linear correction to wave speed. These coefficients are given by

$$c_{i1} = \frac{(\bar{k}_{17} - k_{17})k_{19}}{(k_1 - j_0 k_8)^2 + k_{19}^2} \tag{34}$$

$$c_{i3} = \frac{k_{19}k_{49} + (k_1 - j_0 k_8)k_{48}}{4((k_1 - j_0 k_8)^2 + k_{19}^2)} \tag{35}$$

$$c_{r1} = \bar{c} + \frac{(k_1 - j_0 k_8)(k_{17} - \bar{k}_{17})}{(k_1 - j_0 k_8)^2 + k_{19}^2} \tag{36}$$

$$c_{r3} = \frac{k_{19}k_{48} + (j_0 k_8 - k_1)k_{49}}{4((j_0 k_8 - k_1)^2 + k_{19}^2)}. \tag{37}$$

Finally, equations (32) and (33) are simplified by letting $\varepsilon = 1$.

DISCUSSION

The scaling in the non-linear stability problem (in equations (10)–(14) of ref. [14]) require that mean liquid and vapour velocities be of the same order with respect to α. The solution of the problem based on this scaling (equations (34), (37) and (41) of ref. [14]) introduces F as an important parameter relating the mean vapour and liquid velocities. It is noted that the mean liquid and vapour velocities cannot be independently specified in the statement of the mathematical formulation of the problem. On the contrary, a given mean vapour velocity will establish a corresponding mean liquid velocity. The relationship between Ψ and Φ is explicitly displayed in the solution given in equation (37) of ref. [14]. Specifically, it is found that $\Psi = O(1)$ whenever $\Phi = O(1/F)$ with respect to the acceleration effect parameter, F.

The scaling in ref. [14] further requires that $\gamma\Phi_y \simeq -\alpha^2\Psi_x$. Noting that $\Phi_y \simeq -V\alpha$, $V \simeq j_0$, $j_0 = F/\gamma R$ and that $\Psi_x = O(1)$ with respect to α, it is clear that $F/\alpha R$ is of first order with respect to α. Here, F/R is the slow scale for the base flow and α is the slow scale for the stability problem. This ordering limits the applicability of the non-linear stability results to $|\alpha| \ll 1$, i.e. to long waves. The present results will be inapplicable for short waves and the following discussion will be limited to long waves. The solution to the non-linear stability problem as given by equations (32)–(37) is in dimensionless form and can be utilized to study many special situations. The solution depends on eight parameters α, L, u, Pr, N, F, γ and ϕ. Results will be discussed only for forced vapour flow condensation of saturated steam at 100°C onto an isothermal surface at 53°C. Only three different surface orientations depicted in Fig. 2 will be considered, namely $\phi = 0$, $-90°$, and $90°$. For this practical example $Pr = 2.62$, $N = 12\,347$, $F = 0.0333$ and $\gamma = 0.00061$. In the present study, the linearized part of the stability problem has been simplified by the transformation of the interfacial mass conservation condition (6) into equation (7). As a result, the expression for the linear wave amplification rate given

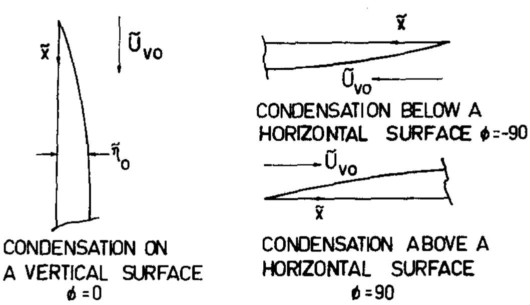

FIG. 2. Vertical and horizontal surface orientations.

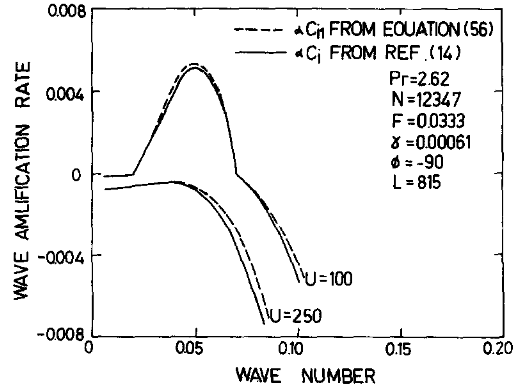

FIG. 3. Linear wave amplification rates for condensation below a horizontal surface.

by equation (34) is an approximation to equation (67) of ref. [14]. In order to test the accuracy of this approximation, αc_{i1} computed from equation (34) is compared with αc_i obtained from equation (67) of ref. [14] in Fig. 3 for condensation below horizontal surfaces. Good agreement between the two predictions for the linear wave amplification rate has been observed for other values of Pr, N, F, γ, and ϕ. A slightly larger discrepancy is observed between the two predictions at larger vapour velocities and smaller density ratios which can be seen by the comparison of Fig. 7 of this study with Fig. 5(a) of ref. [14]. The non-linear wave amplification rate computed from equation (32) for the same physical situation is depicted in Fig. 4. It is observed from this figure that an increase in the dimensionless free stream vapour velocity, U, from 100 to 250 is sufficient to completely stabilize a finite amplitude wave on a condensate film under a horizontal surface and located at a dimensionless distance of $L = 815$ from the leading edge of the isothermal plane surface. Increased vapour velocity has stabilizing effects on both small amplitude disturbances (Fig. 3) and finite amplitude disturbances (Fig. 4) for this example. Linear and non-linear wave amplification rates for cocurrent forced vapour flow condensation at a dimensionless location $L = 815$ from the upper end of an isothermal vertical

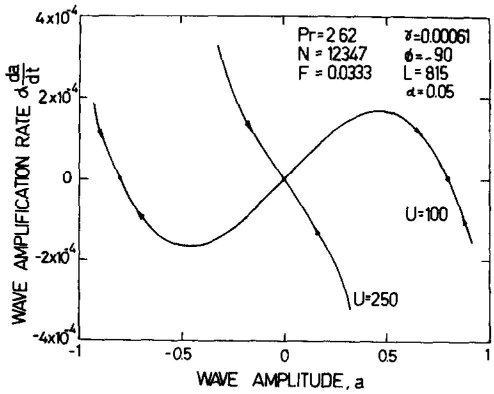

FIG. 4. Wave amplification rates for condensation below a horizontal surface.

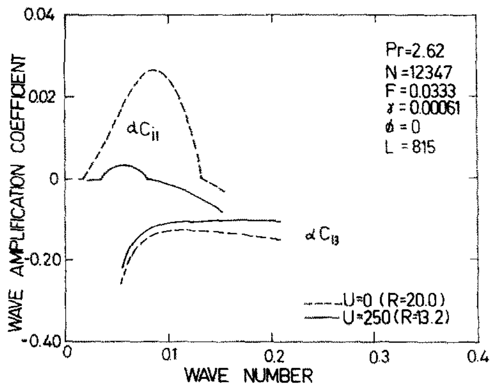

FIG. 5. Linear and non-linear wave amplification coefficients for condensation on a vertical surface.

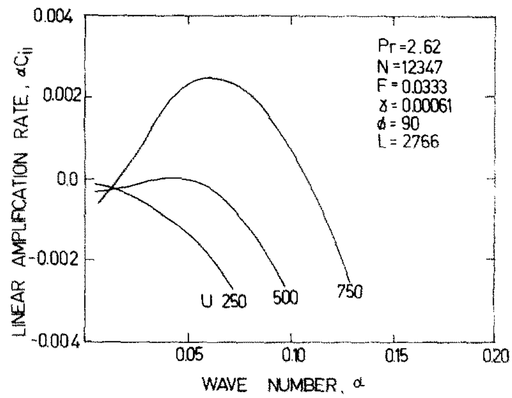

FIG. 7. Linear wave amplification rates for condensation above a horizontal surface.

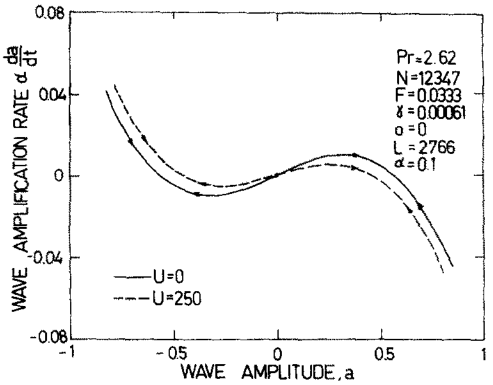

FIG. 6. Wave amplification rates for condensation on a vertical surface.

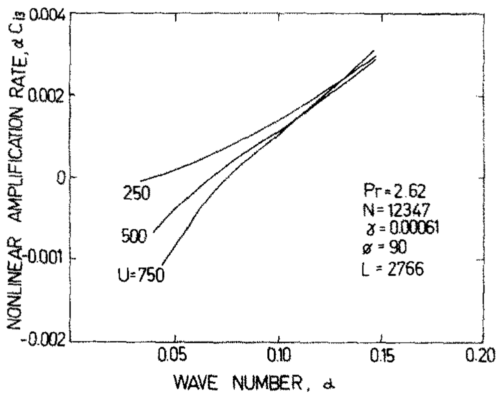

FIG. 8. Non-linear wave amplification coefficient for condensation above horizontal surfaces.

surface are depicted in Fig. 5. The linear wave amplification rate decreases drastically while the non-linear wave amplification rate increases slightly as the dimensionless vapour velocity is increased from 0 to 250. The overall effect decreases the equilibrium wave amplitude by an order of magnitude. Figure 6 shows the wave amplification rate for a finite amplitude disturbance when $\alpha = 0.1$ for the same physical situation when the location on the surface is changed from $L = 815$ to 2766. For this case, the condensate film admits finite amplitude wave motion with large equilibrium amplitudes. Increase of the dimensionless vapour velocity from 0 to 250 tends to decrease the equilibrium wave amplitude.

Non-linear stability characteristics of a disturbance on a condensate film flowing over a horizontal plate and located at a dimensionless distance $L = 2766$ from a leading edge of the plate are considered in Figs. 7 and 8. A finite amplitude disturbance at this location is completely stable when $u = 250$. The linear wave amplification coefficient, αc_{i1}, is positive inside a small wave number band centred about $\alpha = 0.04$ when $u = 500$. The non-linear coefficient, αc_{i3}, is negative inside the same wavelength band. In this case, the condensate film admits supercritically stable finite amplitude wave motion. With further increase of the vapour velocity to $u = 750$ both linear and non-linear amplification coefficients become positive inside the wave number band $0.08 < \alpha < 0.11$ which may be an indication of possible entrainment into the vapour phase. The theoretical analysis presented in this study will lead to results of further practical value when the analysis is extended for the prediction of heat transfer through a wavy condensate film flowing on a surface of arbitrary inclination and adjacent to a forced vapour flow.

REFERENCES

1. J. P. Holman, *Heat Transfer*, p. 434. McGraw-Hill, New York (1981).
2. W. M. Rohsenow, Heat transfer and temperature distribution in laminar-film condensation, *Trans. Am. Soc. Mech. Engrs* **78**, 1945–1948 (1956).
3. E. M. Sparrow and J. L. Gregg, A boundary-layer treatment of laminar film condensation, *J. Heat Transfer* **81**, 13–18 (1959).
4. M. M. Chen, An analytical study of laminar film condensation: Part 1. Flat plates, *J. Heat Transfer* **83**, 48–54 (1961).
5. J. C. Y. Koh, E. M. Sparrow and J. P. Hartnett, The two phase boundary layer in laminar film condensation, *Int. J. Heat Mass Transfer* **2**, 69–82 (1961).
6. I. G. Shekriladze and V. I. Gomelauri, Theoretical study of laminar film condensation of flowing vapour, *Int. J. Heat Mass Transfer* **9**, 581–591 (1966).
7. V. E. Denny and A. F. Mills, Nonsimilar solutions for

laminar film condensation on a vertical surface, *Int. J. Heat Mass Transfer* **12,** 965–979 (1969).
8. J. C. Y. Koh, Film condensation in a forced convection boundary layer flow, *Int. J. Heat Mass Transfer* **5,** 941–954 (1962).
9. S. G. Bankoff, Stability of liquid flow down a heated inclined plane, *Int. J. Heat Mass Transfer* **14,** 337–385 (1971).
10. E. Marschall and C. Y. Lee, Stability characteristics of condensate films, *Wärme- und Stoffübertr.* **1,** 32–37 (1973).
11. M. Ünsal and W. C. Thomas, Linearized stability analysis of film condensation, *J. Heat Transfer* **100,** 629–634 (1978).
12. B. Spindler, Linear stability of liquid films with interfacial phase change, *Int. J. Heat Mass Transfer* **25,** 161–172 (1982).
13. M. Ünsal and W. C. Thomas, Nonlinear stability of film condensation, *J. Heat Transfer* **102,** 483–488 (1980).
14. M. Ünsal, A linearized stability analysis of forced vapor flow condensation, *Proceedings of the NATO-ARW on Advances in Two-phase Flows and Heat Transfer*, F.R.G., 31 August–3 September (1982).
15. M. Ünsal, A closed form solution for average heat transfer coefficient during forced vapour flow condensation on inclined surfaces, *Int. J. Heat Mass Transfer* **31,** 1613–1617 (1988).
16. A. H. Nayfeh, *Perturbation Methods*, Chap. 6. Wiley-Interscience, New York (1973).

APPENDIX A

$$k_{29} = k_4+\alpha k_3$$

$$k_{30} = 4Uk_{16}-3k_5-2U^2k_{13}+6k_{15}$$

$$k_{31} = 3Uk_6+5k_{14}$$

$$k_{32} = 4k_{12}-2Uk_{11}$$

$$k_{33} = k_{16}-2Uk_{13}$$

$$k_{34} = 6Uk_{16}+15k_{15}-U^2k_{13}-3k_5$$

$$k_{35} = 10k_{14}+3Uk_6$$

$$k_{36} = 6k_{12}-Uk_{11}$$

$$k_{37} = 4k_{16}-4Uk_{13}$$

$$k_{38} = k_0-j_0(k_3-k_{29})-j_0k_3(1-2\alpha)-2(k_{30}-j_0^2k_7 -j_0k_{23})+2j_0^2k_6-6k_9+2\bar{c}k_{32}$$

$$k_{39} = -2k_2+2j_0k_{31}-6\bar{c}j_0k_8+2\bar{c}j_0k_{11}+2j_0k_{33}$$

$$k_{40} = k_{38}+2j_0k_3-4j_0k_{20}$$

$$k_{41} = k_{39}+4j_0\bar{c}k_8-4j_0k_{21}$$

$$k_{42} = 2j_0k_3-4j_0k_{20}+k_0-4k_{18}+16k_9+4\bar{c}k_{19}$$

$$k_{43} = 4j_0\bar{c}k_8-4j_0k_{21}-2\bar{c}k_1+2\bar{k}_{17}$$

$$k_{44} = 2k_0-21k_9+\bar{c}k_{32}-k_{30}-j_0(4k_{29}+6\alpha k_3 +j_0k_6+2j_0k_7)$$

$$k_{45} = -2k_2+j_0(3k_{31}-9\bar{c}k_8-3\bar{c}k_{11}-3k_{33})$$

$$k_{46} = -3k_0-3k_9-k_{34}+\bar{c}k_{36}+j_0(2k_{29}+k_3-6\alpha k_3 -k_4+4j_0k_6+3j_0k_7+3j_0k_{13})$$

$$k_{47} = -k_2-j_0(2k_{31}+3\bar{c}k_8+\bar{c}k_{11}-k_{33}-3k_{35}+k_{37})$$

$$k_{48} = b_rk_{44}-b_ik_{45}+k_{46}$$

$$k_{49} = b_ik_{44}+b_rk_{45}+k_{47}$$

$$b_r = (k_{40}k_{42}+k_{41}k_{43})/(k_{42}^2+k_{43}^2)$$

$$b_i = (k_{41}k_{42}-k_{40}k_{43})/(k_{42}^2+k_{43}^2).$$

APPENDIX B

Zeroth-order problem

Differential equation

$$\Phi_{0xx}+\Phi_{0zz} = 0.$$

Boundary conditions at $z = \infty$

$$\Phi_{0x} = \Phi_{0z} = 0.$$

Interfacial energy condition at $z = 0$

$$L_1\eta_0+L_2\Phi_0 = 0$$

where operators L_1 and L_2 are given as follows:

$$L_1 = k_0+k_1\frac{\partial}{\partial T_0}+\bar{k}_{17}\frac{\partial}{\partial x}+k_{18}\frac{\partial^2}{\partial x^2}+k_9\frac{\partial^4}{\partial x^4}+k_{19}\frac{\partial^2}{\partial x\partial T_0}$$

$$L_2 = k_3\frac{\partial^2}{\partial x^2}+k_{20}\frac{\partial^3}{\partial x^2\partial z}-k_{21}\frac{\partial^3}{\partial x^3}-k_8\frac{\partial^3}{\partial x^2\partial T_0}.$$

Interfacial mass condition at $z = 0$

$$\Phi_{0z} = j_0\eta_0.$$

First-order problem

Differential equation

$$\Phi_{1xx}+\Phi_{1zz} = 0.$$

Boundary conditions at $z = \infty$

$$\Phi_{1x} = \Phi_{1z} = 0.$$

Interfacial energy condition at $z = 0$

$$L_1\eta_1+L_2\Phi_1 = -k_1\eta_{0T_1}+k_8\Phi_{0xxT_1}-k_{19}\eta_{0xT_1}-S_2-\Gamma\eta_{0x} +k_0\eta_0^2-2k_2\eta_0\eta_{0x}-k_3\eta_{0x}\Phi_{0x}-k_{29}\eta_{0x}\Phi_{0xz} -k_3\eta_0\Phi_{0xx}-2\alpha k_3\eta_0\Phi_{0xxz}+\frac{\partial}{\partial x}(k_{30}\eta_0\eta_{0x}+k_{31}\eta_0\Phi_{0xx} +k_6\Phi_{0x}\Phi_{0xx}-k_7\Phi_{0z}\Phi_{0xz}+3j_0k_7\eta_0\Phi_{0xz}+3k_8\eta_0\Phi_{0xT_0} -3k_9\eta_0\eta_{0xxx}+k_{32}\eta_0\eta_{0T_0}-k_{11}\eta_{0T_0}\Phi_{0x}+k_{33}\eta_{0x}\Phi_{0x}).$$

Interfacial mass condition at $z = 0$

$$\Phi_{1z} = j_0\eta_1+S_1-j_0\eta_0^2.$$

Second-order problem

Differential equation

$$\Phi_{2xx}+\Phi_{2zz} = 0.$$

Boundary conditions at $z = \infty$

$$\Phi_{2x} = \Phi_{2z} = 0.$$

Interfacial energy condition at $z = 0$

$$L_1\eta_2+L_2\Phi_2 = -k_1\eta_{1T_1}-k_1\eta_{0T_2}+k_8\Phi_{1xxT_1}+S_1k_7\Phi_{0xxz} +k_8\Phi_{0xxT_2}-\Gamma\eta_{1x}-k_{19}\eta_{1xT_1}-k_{19}\eta_{0xT_2}+2k_0\eta_0\eta_1 -2k_2\eta_0\eta_{1x}-2k_2\eta_1\eta_{0x}-3k_3\eta_{1x}\Phi_{0x}-k_3\eta_{0x}\Phi_{1x} -k_{29}\eta_{1x}\Phi_{0xz}-k_{29}\eta_{0x}\Phi_{1xz}-k_3\eta_1\Phi_{0xx}-k_3\eta_0\Phi_{1xx} -2\alpha k_3\eta_1\Phi_{0xxz}-2\alpha k_3\eta_0\Phi_{1xxz}-k_0\eta_0^3-k_2\eta_0^2\eta_{0x} -\alpha k_3\eta_0\eta_{0x}\Phi_{0xz}-\alpha k_3\eta_0^2\Phi_{0xxz}-k_4\eta_0\eta_{0x}\Phi_{0xz}$$

$$+\frac{\partial}{\partial x}(k_{30}\eta_0\eta_{1x}+k_{30}\eta_1\eta_{0x}+k_{31}\eta_1\Phi_{0xx}+k_{31}\eta_0\Phi_{1xx}$$
$$+k_6\Phi_{0x}\Phi_{1xx}+k_6\Phi_{1x}\Phi_{0xx}-k_7\Phi_{0z}\Phi_{1xz}-k_7\Phi_{1z}\Phi_{0xz}$$
$$+3j_0k_7\eta_0\Phi_{1xz}+3j_0k_7\eta_1\Phi_{0xz}+3k_3\eta_0\Phi_{1xT_0}+3k_8\eta_0\Phi_{0xT_1}$$
$$+3k_8\eta_1\Phi_{0xT_0}-3k_9\eta_0\eta_{1xxx}-3k_9\eta_1\eta_{0xxx}+k_{32}\eta_1\eta_{0T_0}$$
$$+k_{32}\eta_0\eta_{1T_0}+k_{32}\eta_0\eta_{0T_1}-k_{11}\Phi_{1x}\eta_{0T_0}-k_{11}\Phi_{0x}\eta_{1T_0}$$
$$-k_{11}\Phi_{0x}\eta_{0T_1}+k_{33}\eta_{0x}\Phi_{1x}+k_{33}\eta_{1x}\Phi_{0x}+k_{34}\eta_0^2\eta_{0x}$$
$$+3k_6\Phi_{0x}\Phi_{0xx}+k_{35}\eta_0^2\Phi_{0xx}-3k_7\eta_0\Phi_{0z}\Phi_{0xz}+3j_0k_7\eta_0^2\Phi_{0xz}$$
$$+3k_8\eta_0^2\Phi_{0xT_0}-3k_9\eta_0^2\eta_{0xxx}+k_{36}\eta_0^2\eta_{0T_0}-2k_{11}\eta_0\eta_{0T_0}\Phi_{0x}$$
$$+k_{37}\eta_0\eta_{0x}\Phi_{0x}-k_{13}\eta_{0x}\Phi_{0x}^2).$$

Interfacial mass condition at $z = 0$

$$\Phi_{2z} = j_0\eta_2-2j_0\eta_0\eta_1+j_0\eta_0^3+j_1\eta_{0T_0}+j_5\eta_{0x}+j_4\Phi_{0xx}-\alpha\Phi_{0zz}.$$

STABILITE NON LINEAIRE DE LA CONDENSATION D'UN ECOULEMENT FORCE DE VAPEUR

Résumé—On étudie par la méthode des échelles multiples la stabilité non linéaire d'un film liquide de condensation s'écoulant sur une surface inclinée isotherme et adjacente à un écoulement de vapeur pure. Les résultats de l'analyse sont discutés dans les cas spéciaux de la condensation d'un écoulement forcé de vapeur sur des surfaces verticales, sous et au-dessus de surfaces horizontales. On trouve que l'accroissement de la vitesse de la vapeur à cocourant a un effet stabilisant sur les films minces de condensat sur des surfaces verticales et sous des surfaces horizontales quand la vitesse de vapeur est faible. On trouve aussi que des films minces coulant au-dessus des surfaces horizontales sous l'action d'une faible vitesse forcée de vapeur à cocourant sont stables vis-à-vis de perturbations infinitésimales ou d'amplitude finie, mais deviennent instables aux grandes vitesses de vapeur.

NICHTLINEARE STABILITÄT BEI DER KONDENSATION IN ERZWUNGENER DAMPFSTRÖMUNG

Zusammenfassung—Es wird die nichtlineare Stabilität eines Kondensatfilms, der auf einer geneigten isothermen Oberfläche fließt und an seinen strömenden Dampf angrenzt, untersucht. Ergebnisse der Untersuchung werden für Spezialfälle erörtert: Für die Kondensation einer erzwungenen Dampfströmung an vertikalen Oberflächen und an der Unter- and Oberseite von horizontalen Flächen. Zunehmende gleichgerichtete Dampfgeschwindigkeit hat auf einen dünnen Kondensatfilm auf einer vertikalen Oberfläche und an einer horizontalen Unterseite einen stabilisierenden Einfluß, solange die Dampfgeschwindigkeiten klein sind. Ein dünner Kondensatfilm, der über eine horizontale Oberfläche fließt, ist unter der Einwirkung gleichgerichteter niedriger erzwungener Dampfgeschwindigkeit stabil. Dies gilt für Störungen mit unendlich kleiner oder auch endlicher Amplitude. Der Film wird jedoch bei höheren Dampfgeschwindigkeiten instabil.

НЕЛИНЕЙНАЯ УСТОЙЧИВОСТЬ КОНДЕНСАЦИИ ПРИ ВЫНУЖДЕННОМ ТЕЧЕНИИ ПАРА

Аннотация—Нелинейная устойчивость пленки жидкого конденсата, натекающей на наклонную изотермическую поверхность и примыкающую к движущемуся потоку беспримесного пара, исследуется методом множественных масштабов. Результаты анализа обсуждаются для конкретных случаев конденсации водяного пара на вертикальных поверхностях, под горизонтальными поверхностями и над ними. Обнаружено, что возрастающая скорость сопутствующего потока оказывает стабилизирующее влияние на тонкие пленки конденсата, стекающие по вертикальным поверхностям и под горизонтальными поверхностями в случае малых скоростей потока пара. Найдено также, что тонкие пленки конденсата, движущиеся над горизонтальными поверхностями под действием сопутствующего низкоскоростного вынужденного потока водяного пара, устойчивы по отношению к возмущениям инфинитеземальной и конечной амплитуд, но становятся неустойчивыми при высоких скоростях пара.